Millisecond annealing for advanced doping of dirty-silicon solar cells

S. Prucnal,[1,a)] B. Abendroth,[2] K. Krockert,[2] K. König,[2] D. Henke,[1] A. Kolitsch,[1] H. J. Möller,[2] and W. Skorupa[1]
[1]*Institute of Ion Beam Physics and Materials Research, Helmholtz-Zentrum Dresden-Rossendorf, P.O. Box 510119, 01314 Dresden, Germany*
[2]*Institute for Experimental Physics, TU Bergakademie Freiberg, Leipziger Str. 23, 09599 Freiberg, Germany*

(Received 18 April 2012; accepted 16 May 2012; published online 19 June 2012)

Cost reduction is the overall goal in the further development of solar cell technologies. Multicrystalline silicon has attracted considerable attention because of its high stability against light soaking. In case of solar grade mc-Si, the rigorous control of metal impurities is desirable for solar cell fabrication. Although ion implantation doping got very recently distinct consideration for doping of monocrystalline solar material, efficient doping of multicrystalline solar material remains the main challenge to reduce costs. The influence of different annealing techniques on the optical and electrical properties of mc-Si solar cells was investigated. Flash lamp annealing (FLA) in the ms-range is demonstrated here as a very promising technique for the emitter formation at an overall low thermal budget. It could be presented that FLA at 1000 °C for 3 ms even without preheating is sufficient to recrystallize implanted silicon. The sheet resistance of FLA samples shows the values of about 50 Ω/sq. Especially, the minority carrier diffusion length for the FLA samples is in the range of 80 μm without surface passivation. This is up to one order of magnitude higher than that observed from rapid thermal annealing or furnace annealing samples. This technology shows great promise to replace the conventional $POCl_3$-doping. © *2012 American Institute of Physics*. [http://dx.doi.org/10.1063/1.4729812]

I. INTRODUCTION

Processing solar cells at lower temperatures helps reducing the energy cost and in thin film technologies may also facilitate the use of less temperature stable substrates, such as normal glass or polymer foils. Poly- and multicrystalline Si films are very important for silicon-gate metal oxide semiconductor integrated circuits, charge-coupled devices, solar cells, thin-film transistors, and various other applications.[1–4] In case of low quality mc-Si containing a relatively high concentration of metal impurities, a low temperature process is desirable for solar cell fabrication. In order to avoid diffusion of metal impurities into the space charge region of the p-n junction, the temperature of the mc-Si substrate should not exceed 400 °C. Another option is the removal of metals from the active area by gettering in the substrate volume far from the p-n junction. Nowadays, the emitter formation for silicon wafer based solar cells is realised by high temperature phosphorous diffusion commonly using a liquid $POCl_3$ source for the dopant. During this furnace annealing (FA) process, metal impurities are gettered at the surface and can be removed afterwards by polishing. For an efficient doping and gettering effect, the samples are annealed at 850–950 °C for at least several minutes. After such a process, the sheet resistance (SR) is in the range of 60 Ohm/sq which ensures good ohmic metal contact formation and the metal impurity concentration in the silicon wafer is reduced by an order of magnitude.[5]

An alternative route to high temperature diffusion for silicon doping is ion implantation followed by short time thermal annealing. In the past, ion implantation had negligible meaning in solar cell production due to low efficiency in large scale mass production. Recently, Varian Solion presented dual-magnet ribbon beam implant architecture for cost-effective high efficiency solar cell production.[6] The key benefit of ion implantation in solar cell manufacturing is cost reduction per watt through process simplification by eliminating phosphosilicate glass (PSG) clean and edge isolation steps. Efficiency of 19% from p-type silicon wafers implanted with phosphorous was announced at the beginning of 2011 by Suniva.[7] However, after phosphorous implantation silicon is partially or totally amorphised depending on the implantation fluence. To recrystallize silicon and activate the dopants, the samples are annealed by rapid thermal annealing (RTA) or FA techniques at temperature usually above 900 °C for a few minutes, what redistributes and activates impurity metals in mc-Si as well. Therefore ion implantation is successfully applied only to n- or p-type monocrystalline silicon.

To extend the application of the ion implantation technique to solar grade (SoG) mc-Si, the diffusion of metal impurities during electrical activation of phosphorous and recrystallization of silicon has to be suppressed. Here, an advanced annealing technique will be presented and explored, which allows the electrical activation of implanted elements by short time light pulse annealing. The flash lamp annealing (FLA) systems are successfully used for silicon recrystallization in many laboratories for applications ranging from ultra-shallow junction formation to recrystallization of amorphous layers.[1,8–12] Leading edge companies as Intel

a)Author to whom correspondence should be addressed. Electronic mail: s.prucnal@hzdr.de.

and AMD have been using it for more than 5 years in shallow junction formation for advanced micro-processor production.[13]

II. EXPERIMENTAL PART

The p-n junctions were formed in multicrystalline SoG p-type silicon wafers by phosphorous implantation and millisecond range FLA. Phosphorous was implanted by conventional ion beam implanter at an energy of 20 kV with fluences of 1.6 and $3.8 \times 10^{15}/cm^2$ corresponding to atomic concentrations of $5 \times 10^{20}/cm^3$ and $1 \times 10^{21}/cm^3$, respectively, with a projected range (R_p) about 30 nm from the surface. Before ion implantation, the texturing of the sample surface by chemical etching was performed. Samples were etched with 40% HF, 65% HNO_3, and 85% H_3PO_4 in the ratio 3:1:3 for about 8 min. In order to electrically activate implanted phosphorous and recrystallized silicon, samples were annealed at 800, 1000, or 1200 °C for 3 or 20 ms with or without preheating. Preheating was done at 400 °C for 1 min. For comparison, standard FA (900 °C, 30 min) and RTA (1000 °C, 30 s) were performed. Structural and optical properties of silicon wafers were investigated by means of μ-Raman spectroscopy and photoluminescence (PL), respectively. The μ-Raman spectra were recorded at room temperature in the backscattering geometry in the range of 150 to 650 cm^{-1} using different laser wavelengths: 325, 442, and 532 nm, resulting in increasing absorption depth and hence extending the information depth from 8 nm to 900 nm below the surface. The PL spectra were recorded at room temperature using the Jobin Yvon Triax 550 monochromator and a cooled InGaAs detector. For the sample excitation during PL measurements, the 532 nm laser light with a power of 200 mW was applied. For the SR measurements, a four-point probe resistor system (CMT-SR 3000 Advanced Instrument Technology) was used. The minority carrier diffusion length was measured by the surface photovoltage spectroscopy (SPV) method. Samples were scanned with six lasers with wavelengths of 785 nm, 809 nm, 850 nm, 904 nm, 950 nm, and 980 nm, corresponding to the penetration depths between 10 and 105 μm. The voltages at each measuring point and wavelength were recorded six times and averaged. The average values are subsequently used to calculate L_D via Goodman plots.

III. RESULTS AND DISCUSSION

Phosphorous ion implantation was used for the solar cell emitter formation in multicrystalline SoG p-type silicon wafers. After ion implantation, the silicon is strongly disordered or amorphous within the ion range. Therefore, subsequent annealing is required to remove the implantation damage and to activate the doping element. The phosphorous implanted and annealed SoG mc-Si wafers were characterised by means of μ-Raman spectroscopy, photoluminescence, four-point probe resistance measurements, and SPV. The influence of the annealing times and temperatures on the optical, microstructural, and electrical properties of p-type mc-Si based solar cell emitters is investigated.

The crystal quality of the silicon wafer after phosphorous implantation and annealing was controlled by Raman spectroscopy. It is well known that ion implantation into a crystalline matrix introduces severe radiation damage and for high doses even amorphization of the implanted region takes place. The recrystallization evolution with depth after various post-implantation annealing was investigated by μ-Raman spectroscopy using different excitation wavelengths (325, 442, and 532 nm). Depending on the excitation wavelength, Raman spectra are recorded from different depth regions. The penetration depth of laser light for 325, 442, and 532 nm in silicon is in the range of 8, 200, and 900 nm, respectively.[14] Hence, after excitation with ultraviolet (UV) (325 nm), blue (442 nm), and green (532 nm) lasers the Raman spectra deliver information about the surface quality, the damaged region due to ion implantation, and bulk material, respectively. Fig. 1 shows the Raman spectra obtained from phosphorous implanted and annealed samples. The spectra from as-implanted samples are shown as well.

Independent of the excitation wavelength, the Raman spectra of as-implanted samples show a broad band at around 470 cm^{-1} related to amorphous silicon.[15] The projected range for implanted phosphorus at 20 keV is around 30 nm from the silicon surface. Hence, taking into account the Gaussian distribution of P atoms, the degradation layer of the silicon due to ion implantation can extend up to 100 nm. Because the penetration depth of the blue and green laser light in amorphous silicon is slightly longer than the

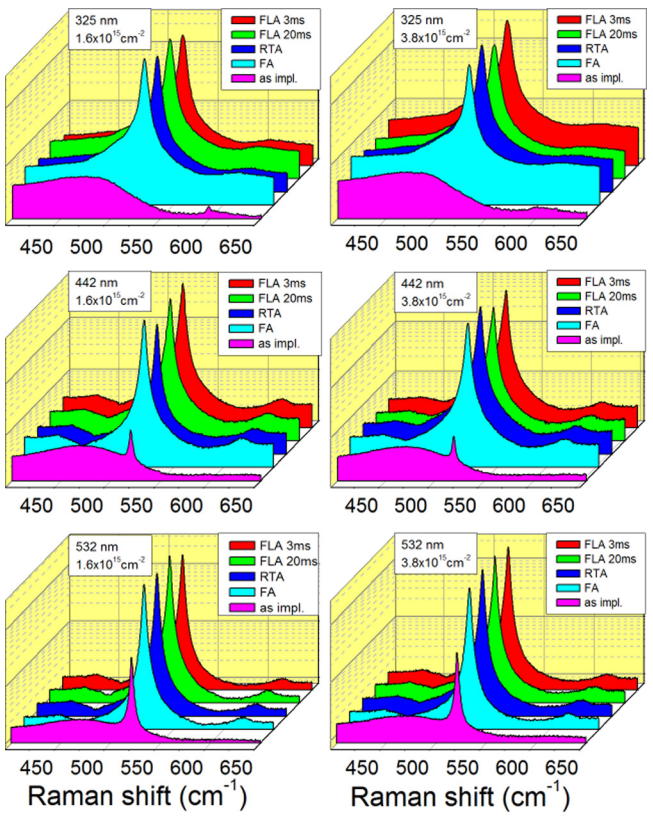

FIG. 1. μ-Raman spectra from implanted and annealed samples after different laser excitation. Annealing conditions: FA-900 °C for 30 min, RTA-1000 °C for 30 s, FLA-1000 °C for 3 or 20 ms with preheating at 400 °C for 1 min.

implantation depth, the small peak visible at 520 cm^{-1} in the as-implanted sample is due to photons scattered from the crystalline silicon substrate. After annealing, there is no significant difference in the Raman spectra between samples annealed at different conditions for both low and high implantation doses. The silicon peak in Raman spectra (520 cm^{-1}) obtained after UV excitation is not symmetric at the low frequency side. The asymmetry of the 520 cm^{-1} peak can be due to:

(1) Silicon was not fully recrystallized during annealing and a residual amorphous phase exists near the surface region.
(2) The surface region contains partially disordered silicon due to a high amount of phosphorous incorporated into the silicon matrix.
(3) Fano interaction as a consequence of interference between discrete phonons and the continuum of electronic states in heavily phosphorous doped Si.[16]

Taking into account that the regrowth rate of damaged silicon is in the range of 1 nm/s at 600 °C and increases rapidly with temperature, the FA (900 °C, 30 min) and RTA (1000 °C, 30 s) samples should not contain the amorphous phase up to the surface.[17] Therefore, the existence of amorphous silicon after annealing independent of the annealing time can be neglected. Hence, we can conclude that the asymmetry of the silicon peak is mainly due to the Fano effect. The broad peak observed at around 618 ± 3 cm^{-1} is designated to the Si-B vibration mode (see Fig. 1).[18] Its intensity and position depend on the free carrier concentration, i.e., boron atoms in substitutional position. With increasing boron concentration, the peak position shifts towards higher wavenumbers.[18] For UV excited samples, only the surface region up to 10 nm contributes to the Raman spectra. For this, the substitutional boron related peak is detected at 615 cm^{-1} and a strong asymmetry of the 520 cm^{-1} Si peak on the low energy side of maximum is observed. By increasing the excitation wavelength to 442 or 532 nm when more bulk material contributes to the Raman spectra, the peak position of the Si-B vibration mode shifts to 618 cm^{-1} and 620 cm^{-1}, respectively. This means that within the implanted region P atoms are in substitutional position after annealing overcompensating positive intrinsic carriers. Furthermore, these results confirm that the FLA in the ms range is sufficient to recrystallize silicon and activate implanted phosphorous.

Figures 2(a) and 2(b) show room temperature photoluminescence obtained from implanted and annealed samples. For PL measurements, the green laser with 532 nm wavelength and 200 mW power was used with an incident angle of 60° to the normal. The broad peak at around 1140 nm corresponds to the band-to-band (B-B) transition in silicon. The side band of the B-B with a maximum at around 1220 nm corresponds to the luminescence centers formed by substitutional phosphorous atoms. The PL intensity strongly depends on the crystal quality of the silicon matrix. Defects, such as atom displacements, vacancies, dangling bonds, etc., work as non-radiative channels for PL de-excitation and hence reducing the PL efficiency. It is worth noting that

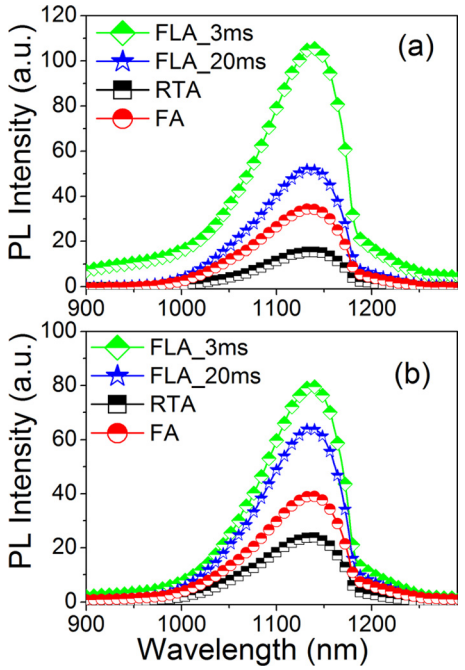

FIG. 2. Room temperature PL spectra obtained from phosphorous implanted with a fluence of 1.6×10^{15} cm^{-2} (a) and 3.8×10^{15} cm^{-2} (b) and annealed samples during 532 nm excitation with 200 mW power. Annealing conditions: FA-900 °C for 30 min, RTA-1000 °C for 30 s, FLA-1000 °C for 3 or 20 ms with preheating at 400 °C for 1 min.

many of these defects cannot be detected in the Raman spectrum but are easily visible in PL measurements. Independent of the implantation fluence, the highest B-B PL intensity was observed from samples annealed for 3 ms and the lowest one for RTA. In our experiments, we have used solar grade mc-Si with a relatively high concentration of metal impurities. During long time annealing (RTA or FA), metals diffuse from the bulk towards the space charge region and are active there as non-radiative recombination centers and carrier traps. Both lead to a decreasing PL intensity and finally kill the photovoltaic effect. During the millisecond range annealing, the thermal budget introduced to the sample is sufficient to activate implanted phosphorous but too short for the diffusion of metal impurities.

An important parameter for the solar cell performance is the sheet resistance of the emitter. From the application point of view, it should be as low as possible in order to provide an ohmic contact between the metal electrode and silicon. Figure 3 presents the average sheet resistance value as a function of different annealing conditions from samples implanted with phosphorous fluences of $1.6 \times 10^{15}/cm^2$ (a) and $3.8 \times 10^{15}/cm^2$ (b). Each sample was measured in 20 points. The lowest SR value is obtained by long time annealing. Values of 27 and 35 Ω/sq for high fluence and 48 and 62 Ω/sq for low fluence implantation were measured for FA and RTA, respectively. The standard deviation of the average SR is in the range of 1.5% for both annealing types. In case of FLA sample, the SR is in the range of 80 ± 10 and 60 ± 6 Ω/sq for low and high fluence of phosphorous, respectively. The standard deviation of the average SR value within the single FLA sample is below 2%.

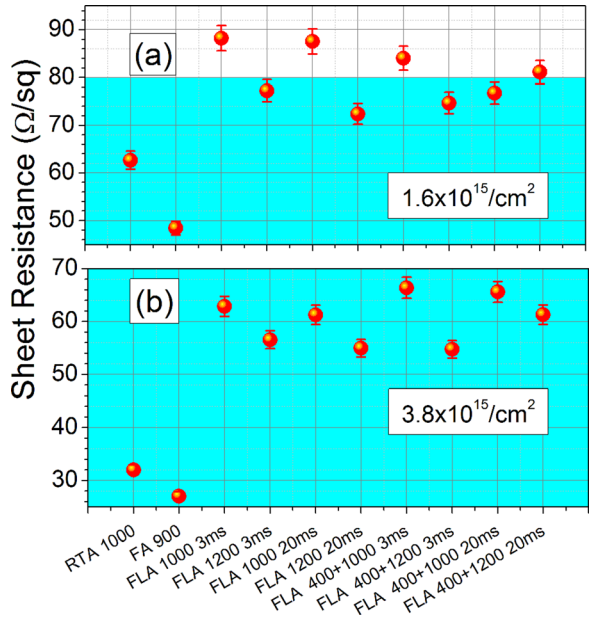

FIG. 3. Sheet resistance measurements as a function of the annealing temperature of the P^+ implanted and annealed mc-Si wafer with a fluence of $1.6 \times 10^{15}/cm^2$ (a) and $3.8 \times 10^{15}/cm^2$ (b). Results in blue area are sufficient for solar cell production.

Independent of the fluence of phosphorous implantation, the lowest minority carrier diffusion length is measured for FA or RTA annealed samples, where L_D is in the range of 5 and 10 μm, respectively (see Figs. 4(a) and 4(b)), unacceptable for solar cell devices. Strong enhancement of L_D was observed after millisecond range annealing for both implantation fluences. In comparison with standard annealing, a more than twofold increase of L_D was observed from samples annealed at 1200 °C for 3 or 20 ms. For the annealing temperature of 1000 °C for 3 ms, the minority carrier diffusion length was one order of magnitude higher than observed for FA samples. Simultaneously, the PL intensity value of FLA samples at 1000 °C for 3 or 20 ms is the best and the SR value is in the range typically used in solar cell device formation.

Figs. 4(c)–4(e) show the SPV scan of 3×3 cm^2 area from samples implanted with a fluence of 1.6×10^{15} P^+/cm^2 and annealed at 900 °C for 30 min (c), 1000 °C for 30 s (d), and 1000 °C for 3 ms with 400 °C preheating for 1 min (e). The average L_D for 3×3 cm^2 area is 9.55 μm for FA, 9.13 μm for RTA, and 67.92 μm for FLA. The inhomogeneity of the average L_D determined from SPV measurements is in the same range for all samples and does not exceed 10%. It is worth noticing that the SPV measurements were performed on not optimised samples. Further increase of the L_D can be obtained by hydrogen passivation of defects and SiN layer deposition as antireflection coating. The application of the FLA technique in the low-cost solar cell production is an alternative route for the metal-impurity engineering proposed by Buonassisi *et al.*[19] or standard phosphorous gettering.[20] Buonassisi *et al.* have shown an influence of the cooling rate on the metal impurity distribution in mc-Si. Slowly cooled samples exhibit a low density of micrometre size defect clusters and a fourfold increase of L_D (up to 50 μm) in comparison with fast cooled samples.[19] In our case, the FA and RTA annealed samples show the L_D in the same range as that obtained by Buonassisi *et al.* for fast cooled samples (around 10 μm) and up to two times higher value after FLA comparable to those of slowly cooled mc-Si.

IV. CONCLUSIONS

In summary, we have shown that the FLA is a unique technique applicable for the multicrystalline solar grade silicon photovoltaic cell production. Within the millisecond annealing time, implanted phosphorous is electrically

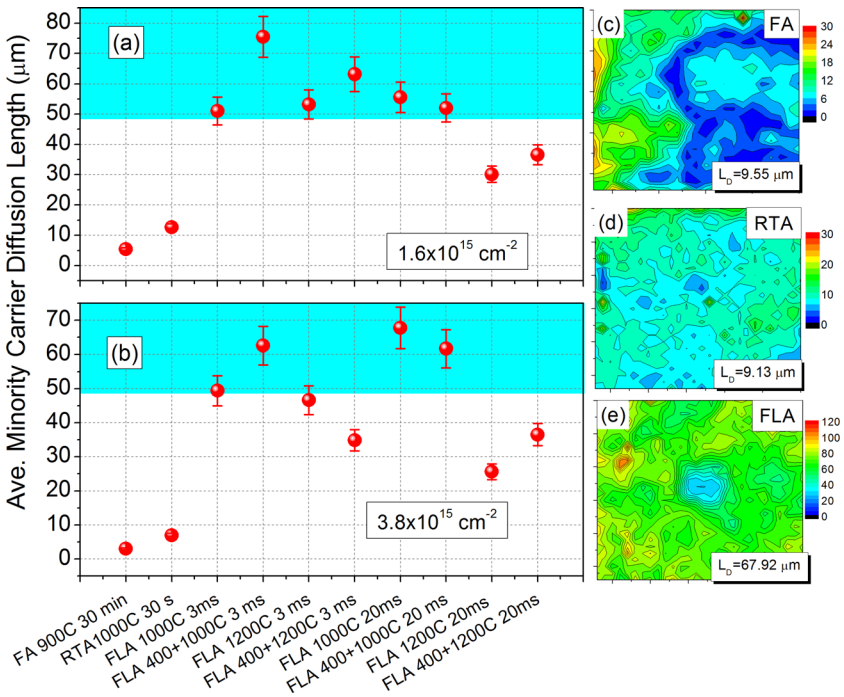

FIG. 4. Average minority carrier diffusion length for different annealing conditions obtained from mc-Si implanted with a fluence of 1.6×10^{15} (a) and 3.8×10^{15} P^+/cm^2 (b) after line SPV scan. SPV scan of 3×3 cm^2 samples implanted with a fluence of 1.6×10^{15} P^+/cm^2 and annealed at 900 °C for 30 min (c), 1000 °C for 30 s (d), and 1000 °C for 3 ms with 400 °C preheating for 1 min (e). Results in blue area are sufficient for solar cell production.

activated and silicon is recrystallized. Simultaneously, the diffusion of metal impurities and their activation is suppressed. The combination of ion implantation and FLA reduces the solar cell fabrication steps by two (PSG clean and edge isolation) leading to significant cost reduction. The next step is to employ plasma-based ion implantation for phosphorous doping, which may further simplify the solar cell preparation.

ACKNOWLEDGMENTS

This work was performed within the Cluster of Excellence "Structure Design of Novel High-Performance Materials via Atomic Design and Defect Engineering (ADDE)" that is financially supported by the European Union Regional Development Funds and by the Ministry of Science and Art of Saxony (SMWK).

[1]K. Ohdaira, T. Fujiwara, Y. Endo, K. Shiba, H. Takemoto, and H. Matsumura, Jpn. J. Appl. Phys. **49**, 04DP04 (2010).
[2]H. Watanabe, H. Miki, S. Sugai, K. Kawasaki, and T. Kioka, Jpn. J. Appl. Phys. **33**, 4491–4498 (1994).
[3]A. Suboundji, T. Mohammed-Brahim, G. Andrä, J. Bergmann, and F. Falk, J. Non-Cryst. Solids **338–340**, 758–761 (2004).
[4]N. K. Mudugamuwa, A. Adikaari, D. Dissanayake, V. Stolojan, and S. Silva, Sol. Energy Mater. Sol. Cell **92**, 1378–1381 (2008).
[5]I. Périchauda, S. Martinuzzia, J. Degoulangeb, and C. Trassy, Mater. Sci. Eng., **159–160B**, 256–258 (2009).
[6]J. Benic, N. Bateman, and M. Hermle, paper presented at the 25th European PV Solar Energy Conference and Exhibition, Valencia, Spain, 5–10 September 2010.
[7]A. Rohatgi, D. L. Meier, B. McPherson, Y.-W. Ok, A. D. Upadhyaya, J.-H. Lai, and Francesco Zimbardi, Energy Procedia **15**, 10–19 (2012).
[8]B. Pécz, L. Dobos, D. Panknin, W. Skorupa, C. Lioutas, and N. Vouroutzis, Appl Surf. Sci. **242**, 185–189 (2005).
[9]W. Skorupa, T. Gebel, R. A. Yankov, S. Paul, W. Lerch, D. F. Downey, and E. A. Arevalo, J. Electrochem. Soc. **152**, G436–G440 (2005).
[10]F. Terai, S. Matunaka, A. Tauchi, Ch. Ichimura. T. Nagatomo, and T. Homma, J. Electrochem. Soc. **153**, H147–H150 (2006).
[11]Ch. H. Poon, A. See, Y. Tan, M. Zhou, and D. Gui, J. Electrochem. Soc. **155**, H59–H63 (2008).
[12]W. Anwand, S. Z. Xiong, C. Y. Wu, T. Gebel, Th. Schumann, G. Brauer, and W. Skorupa, Acta Phys. Pol. A **113**, 1273–1278 (2008).
[13]S. Govindaraju, C.-L. Shih, P. Ramanarayanan, Y.-H. Lin, and K. Knutson, ECS Trans. **28**, 81–90 (2010).
[14]D. E. Aspens and A. A. Studna, Phys. Rev. B **27**, 985–1009 (1983).
[15]J. E. Smith, Jr., M. H. Brodsky, B. L. Crowder, M. I. Nathan, and A. Pinchuk, Phys. Rev. Lett. **26**, 642–646 (1971).
[16]U. Fano, Phys. Rev. **124**, 1866–1878 (1961).
[17]N. G. Rudawski, K. S. Jones, S. Morarka, M. E. Law, and R. G. Elliman, J. Appl. Phys. **105**, 081101 (2009).
[18]R. Beserman and T. Bernstein, J. Appl. Phys. **48**, 1548–1550 (1977).
[19]T. Buonassisi, A. A. Istratov, M. A. Marcus, B. Lai, Z. Cai, S. M. Heald, and E. R. Weber, Nature Mater. **4**, 676–679 (2005).
[20]M. Loghmarti, K. Mahfoud, J. Kopp, J. C. Muller, and D. Sayah, Phys. Status Solidi A **151**, 379–386 (1995).